The Third Fuel & Combustion Conference of IRAN

Tehran - IRAN Feb. 2010

Iranian Combustion Institue

Amirkabir Univ. of Technology
Aerospace Engineering Dept.

FCCI2010-1160

Radiation, Diffusion and Kinetics Effects on NO_X Formation in Non-Sooting Oxygen-Enhanced Flamelets

Hamid Hashemi[*,§], Mohammad Ali Soroudi[**] and Karim Mazaheri[***]
[*] Research Assistant, Department of Aerospace Engineering, Sharif University of Technology
[**] Research Assistant, Department of Aerospace Engineering, Sharif University of Technology
[***] Professor, Department of Aerospace Engineering, Sharif University of Technology

([§]hamid1981@gmail.com)

ABSTRACT In this work, effects of thermal radiation, chemical kinetics, and molecular diffusion models on NO_X formation in non-sooting oxygen-enhanced counterflow flamelets have been studied numerically. Thermal radiation is included via optically thin radiation model. Three different reaction mechanisms including GRI 2.11, GRI 3.0, and San Diego mechanisms were used. Molecular diffusion effects have been investigated with multicomponent and mixture-averaged transport models. Additionally, thermal diffusion effects (Soret effect) were investigated. Numerical results were compared with published data of Raman scattering measurements of major species, and linear laser-induced fluorescence and laser-saturated fluorescence measurements of thermal NO. The numerical results show acceptable agreement with experimental data. Results indicated that maximum value of NO reduced noticeably in case radiation has been considered. In general, including radiation effects produced more accurate results. Among various reaction mechanisms, GRI 3.0 shows better agreement while it still overpredicted NO. Finally, it has been shown that implementation of multicomponent diffusion model with Soret effect resulted in best outcome comparing to experimental data.

Keywords Oxygen-enriched combustion, Thermal radiation, Molecular diffusion, Chemical kinetics, NO_X emissions.

INTRODUCTION

Oxygen-enhanced or oxygen-enriched combustion (OEC) has been used increasingly in industry over the last two decades to improve productivity and reduce emissions [Baukal 1999]. Unlike traditional combustion, oxygen-enhanced combustion has oxygen concentration varying from 21% to 100% and when 100% O_2 is used as the oxidizer, it is termed an oxy-fuel flame. Recently the DOE has proposed oxygen-enriched combustion with carbon sequestration as a means of reducing greenhouse gases [NETL Report 2004]. The fundamental effects of oxygen-enrichment on flame characteristics are high flame temperature, high flame speed, reduced flame length and increased flammability range [Cheng et al. 2006].

Kuligowski and Laurendeau [1997] studied the influence of oxygen enrichment on NO_X production for a coflow diffusion flame burning pure methane. They found that the NO_X emission index ($EINO_X$) peaked at about 60% O_2 content in the oxidizer and that over 95% O_2

content was needed to give $EINO_X$ values less than those obtained when using air as the oxidizer.

Sung and Law [1998] studied NO production in counterflow diffusion flames under conditions of oxygen enhancement using an elementary chemical kinetic model. They found that the effect of N_2 on the oxidizer side of a diffusion flame was more problematic than that on the fuel side and that thermal NO dominates in diffusion flames having high oxygen contents. Beltrame et al. [2001] computationally studied both NO and soot formation under conditions of oxygen enrichment in counterflow diffusion flames by using detailed chemical kinetic models. In agreement with Sung and Law [1998], they found that thermal NO dominates under these conditions. They also found that soot formation is enhanced and that the sooting zone becomes narrower with an increase in oxygen content.

Naik and Laurendeau [2002a] reported quantitative, spatially resolved linear laser-induced fluorescence (LIF) and laser-saturated fluorescence (LSF) measurements of thermal NO in high-temperature, oxygen-rich, counterflow diffusion flames at atmospheric pressure. The results for these non-sooting flames indicated excellent agreement between measured and predicted NO concentrations. A comparison of linear LIF and LSF measurements also yielded excellent agreement. Subsequently, Naik and Laurendeau [2002b] reported quantitative, spatially resolved, laser-saturated fluorescence measurements of NO in high-temperature, oxy-fuel, counterflow sooting diffusion flames at atmospheric pressure. LSF measurements were compared to numerical predictions and comparisons of measurements with predictions indicated good agreement in those regions of the flames for which the temperatures were below 2600 K. Excellent spatial agreement was also observed because of dominance by the well-known thermal mechanism. However, poorer agreement was found between predicted and measured NO in central regions of these flames at higher temperatures. Naik et al. [2003] studied the effect of soot radiation on NO formation in laminar, counterflow, $CH_4/O_2/N_2$ oxy-fuel flames by varying the N_2 content in both the oxidizer and fuel streams. Quantitative LSF measurements of NO have been compared to predictions obtained by considering gas-phase radiation, both without and with soot radiation. Comparisons of NO measurements with computations indicated excellent agreement in regions of the flames for which temperatures are below 2600 K. However, some disagreement is observed at higher temperatures near peak NO locations, although the inclusion of a soot formation and radiation model improves the agreement.

Wang et al. [2005] developed a computational fluid dynamics (CFD) model of oxygen-enriched turbulent flames by integrating state-of-the-art models for detailed hydrocarbon oxidation and NO_X chemistry, soot formation and oxidation, and thermal radiation into a three-dimensional unstructured CFD code. Results showed that soot and spectrally radiating gas-phase species are distributed separately in the flame, and this segregation of radiating media strongly affects the radiant heat flux, flame structure, flame temperature, and NO_X emissions. Cheng et al. [2006] investigated planar oxygen-enhanced methane counterflow flames by optical diagnostics and numerical simulation with two different reaction mechanisms. The major species concentrations and temperature measured from Raman scattering are compared to the detailed simulations of the flame formed between two opposed jets. The effect of stretch and the influence of oxygen concentration in the oxidizer on the flame structure studied for nitrogen-diluted methane fuel.

The oxygen concentration of reactants changes the flame temperature dramatically. The effect of the fuel concentration in the nitrogen-diluted fuel is also studied for pure oxygen flames.

Theoretically, NO_X can be eliminated by oxy-fuel combustion. Unfortunately in practical systems, a small percentage of N_2 always exists in the fuel (due to impurities in the fuel supply) or oxidizer (due to furnace leaks and the failure to maintain a positive pressure in the combustor and feeding streams) and NO_X emissions can be worse because of thermal NO_X formation at high temperature in the oxygen-enhanced flames. Therefore, detailed numerical modeling of NO_X formation in oxygen-enhanced combustion with various levels of nitrogen contamination is needed for development of oxy-fuel combustion technology. The focus of this work is on investigation of nitric oxide formation in laminar counterflow flamelets of methane under non-sooting oxygen-enhanced conditions. Studies of strained laminar opposed-flow diffusion flames (i.e. counterflow flamelets) have been extensively applied to develop a fundamental understanding of flame structure and extinction [Williams 2000]. Recently, authors of this work used counterflow flamelet configuration to study some fundamental aspects of natural gas combustion [Soroudi et al. 2006; Hashemi et al. 2009]. In this work, effects of thermal radiation, different chemical kinetics mechanisms, and various molecular diffusion models on NO_X formation in non-sooting oxygen-enhanced counterflow flamelets have been studied.

PHYSICAL MODEL AND NUMERICAL SOLUTION

In this paper, we study the effects of oxygen enhancement in non-sooting counterflow non-premixed flames. In this configuration, by using two axisymmetric tubular opposite nozzles, two flows have been leaded to encounter and make a stagnation plane, on which axial velocity vanishes. This geometry makes an attractive experimental configuration, because the flame is flat, allowing for detailed study of the flame chemistry. Some simplifications convert this three dimensional problem to a one dimensional problem which could be solved more easily. Main assumption is that the radial component of velocity is linear in radius so the dependent variables become functions of the axial direction only [Kee et al. 2003].

Equations were written in the cylindrical coordinate for more convenience. Steady state conservation of mass equation [Kee et al. 2003]:

$$\frac{\partial(\rho u)}{\partial x}+\frac{1}{r}\frac{\partial(r\rho v)}{\partial r}=0 \qquad (1)$$

Considering mentioned assumption, that the radial component of velocity is linear in radius, we define:

$$G(x)=\frac{\rho v}{r},\quad F(x)=\frac{\rho u}{2} \qquad (2)$$

So, mass equation was reduced to:

$$G(x)=\frac{dF(x)}{dx} \qquad (3)$$

H, reduced radial pressure gradient, remains constant:

$$H = \frac{\partial P}{r \partial r} \tag{4}$$

Perpendicular momentum equation:

$$H - 2\frac{d}{dx}(\frac{FG}{\rho}) + \frac{3G^2}{\rho} + \frac{d}{dx}[\mu \frac{d}{dx}(\frac{G}{P})] = 0 \tag{5}$$

Energy equation:

$$\rho u \frac{dT}{dx} - \frac{1}{C_P}\frac{d}{dx}(\lambda \frac{dT}{dx}) + \frac{\rho}{C_P}\Sigma(C_{P,k} Y_k V_k)\frac{dT}{dx} + \frac{1}{C_P}\Sigma(h_k \dot{\omega}_k) = 0 \tag{6}$$

Conservation of species:

$$\rho u \frac{dY_k}{dx} + \frac{d}{dx}(\rho Y_k V_k) - \dot{\omega}_k W_k = 0 \tag{7}$$

Diffusion velocities can be computed by multicomponent or mixture-averaged formulation. Multicomponent formula usually results in more accuracy:

$$V_k = \frac{1}{X_k \overline{W}} \sum_{j \neq k}^{K} W_j D_{k,j} \frac{dX_j}{dx} - \frac{D_k^T}{\rho Y_k}\frac{1}{T}\frac{dT}{dx} \tag{8}$$

But more computational time will be needed for multicomponent model. Therefore, to reduce computation efforts, sometimes mixture averaged formula is being used:

$$V_k = -\frac{1}{X_k} D_{km} \frac{dX_k}{dx} - \frac{D_k^T}{\rho Y_k}\frac{1}{T}\frac{dT}{dx} \tag{9}$$

Where,

$$D_{km} = \frac{1 - Y_k}{\sum_{j \neq k}^{K} \frac{X_j}{\Delta_{jk}}} \tag{10}$$

Boundary conditions for the fuel and oxidizer streams at the nozzles exits:

$$x = 0 \rightarrow \begin{cases} \mathrm{F(x)} = \frac{\rho_F u_F}{2},\ \mathrm{G(x)} = 0, \mathrm{T} = \mathrm{T_F}, \\ (\rho \mathrm{u Y_k}) + (\rho \mathrm{Y_k V_k}) = (\rho \mathrm{u Y_k})_F \end{cases}$$

$$x = L \rightarrow \begin{cases} \mathrm{F(x)} = \frac{\rho_O u_O}{2}, \mathrm{G(x)} = 0, \mathrm{T} = \mathrm{T_O}, \\ (\rho \mathrm{u Y_k}) + (\rho \mathrm{Y_k V_k}) = (\rho \mathrm{u Y_k})_O \end{cases} \tag{11}$$

Global strain rate has a significant role in counterflow flame structure [Cheng et al. 2006]:

$$a_s = \frac{2|u_O|}{L}(1 + \frac{|u_F|}{|u_O|}\sqrt{\frac{\rho_F}{\rho_O}}) \tag{12}$$

By specifying a_s, applying momentum balance for gases at nozzles, and implementing ideal gas state equation, velocities and all properties at each nozzle exit could be calculated:

$$\rho_O u_O^{\,2} = \rho_F u_F^{\,2} \quad (13)$$

$$Pv = RT \quad (14)$$

To consider effect of radiation on flame structure, an optically thin radiation model is employed. In this model, heat flux computed by this equation [Barlow et al. 2001]:

$$q = 4k_p\sigma(T^4 - T_\infty^{\,4}) \quad (15)$$

Where,

$$k_p = \Sigma(k_{p,k}X_k P) \quad (16)$$

Planck mean absorption coefficients ($k_{p,k}$) for CO_2 and H_2O are calculated using Chemkin-III data expressed as functions of temperature. The optically thin assumption should yield a good approximation of the true radiative effects in these types of flames [Barlow et al. 2001].

To solve above equations, we used OPPDIF program from Chemkin-III collection [Kee et al. 2003]. This program initially has been developed by Sandia National Laboratory, and can simulate premixed/non-premixed counterflow flames. Our survey on reaction mechanisms included three ones: GRI-Mech versions 2.11 and 3.0 [Bowman et al. 1999], and San Diego reaction mechanism for small hydrocarbons [Williams 2005].

GRI-2.11 includes 279 elementary reactions and 49 species to simulate methane and natural gas combustion. GRI-3.0 was presented in 1999 and includes 325 elementary reactions and 53 species. The last version of San Diego mechanism which focused on combustion of a relatively wide range of light hydrocarbons by considering 46 species and 235 elementary reactions has been released in 2005. This mechanism doesn't include NOx chemistry by default but a supplementary mechanism [Williams 2005] to simulate nitrogen chemistry is available and is added to main mechanism in this work.

RESULTS AND DISCUSSION

Validation In all simulations in this work, pressure was set to one atmosphere. Additionally, by using adaptive re-gridding and controlling relevant values of GRAD and CURV parameters, we obtained a suitable grid to solve the problems. In all cases, values of GRAD and CURV are set to 0.1 to ensure fine grid and independency of results from the grid. Furthermore, except when mentioned, all simulations are performed with enabling Optically Thin Radiation (OTM) model to simulate radiation effect and multicomponent model with Soret effect to simulate diffusion properties in OPPDIF program.

For validation of used model and numerical simulation, we compared our numerical results to what was published by Cheng et al. [2006]. They manipulated an optical diagnostic method, nonintrusive Raman scattering system, to investigate effect of enhanced oxygen on combustion of methane. For better verification, we choose two cases from their work, one near reported extinction and another far away extinction. Table 1 includes parameters and configurations of

flames that have been used in this study. As it seems clear in Fig 1, numerical simulation by using GRI 3.0 reaction mechanism can predict temperature behavior in both flames fairly well. In addition, O_2, CO_2, and H_2O show acceptable agreement. In Fig 1, all experimental data seems to be shifted slightly toward oxidizer side. It is possibly because of some uncertainty in measuring horizontal position in experimental setup.

In Fig 2 showing data of flame C2, this discrepancy in horizontal location estimation faded noticeably. In general, serious errors in numerical simulations have not been observed and results are satisfying.

Table 1
Flame parameters

Flame index	Stretch rate, a_s (s^{-1})	Temperature at nozzles(K)	Distance between nozzles (cm)	Fuel side (Molar fractions)		Oxidizer side (Molar fractions)	
				CH_4	N_2	O_2	N_2
C1	60	300	1.26	20%	80%	30%	70%
C2	60	300	1.26	8%	92%	100%	0.0%
C3	37.69	300	2.0	25%	75%	100%	0.0%
C4	37.14	300	2.0	50%	50%	50%	50%
C5	34.77	300	2.0	100%	0.0%	35%	65%

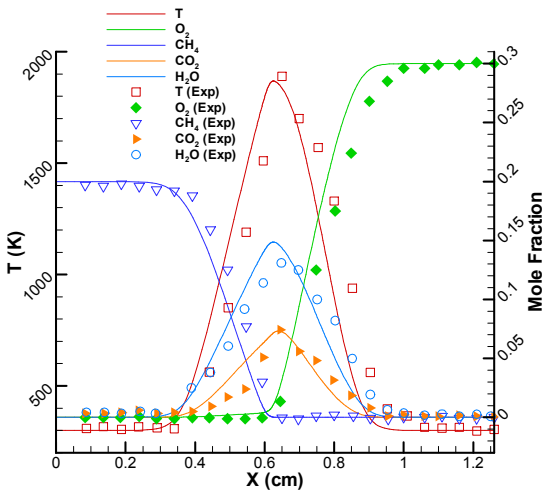

Figure 1. Temperature and major species variation with distance from fuel side for flame C1. Lines represent numerical results of simulation by GRI 3.0 mechanism and symbols represent experimental results of Cheng et al. [2006].

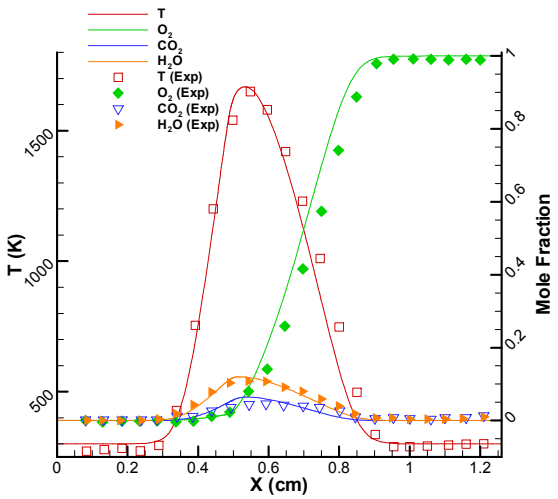

Figure 2. Temperature and major species variation with distance from fuel side for flame C2. Lines represent numerical results of simulation by GRI 3.0 mechanism and symbols represent experimental results of Cheng et al. [2006].

Effect of Radiation After sureness of suitability and accuracy of applied reaction mechanisms and numerical method, we investigated effects of radiation on overall structure and NO production in flames. Fig 3 shows effects of radiation on temperature profile for flame C3. As expected, radiation decreases maximum temperature of flames. To investigate effect of radiation on NO production, we compared numerical results to experimental ones that were published by Naik et al. [2002a]. They used two different methods, LIF and LSF, to measure NO in non-sooting oxygen enriched conditions. Fig 4 presents numerical results in both radiative and adiabatic cases and mentioned experimental results. Maximum value of NO occurring at flame

front reduced noticeably in case radiation has been considered. However, both numerical models overestimate NO while both experimental methods show nearly identical results. Higher value for NO in adiabatic case might be result of higher temperature and consequently more production of NO because of thermal mechanism.

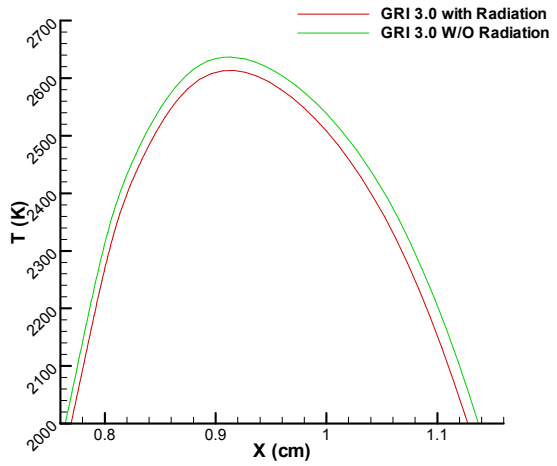

Figure 3. Temperature variation with distance from fuel side for flame C3. Lines represent numerical results of simulation by GRI 3.0 mechanism in both radiative and adiabatic cases.

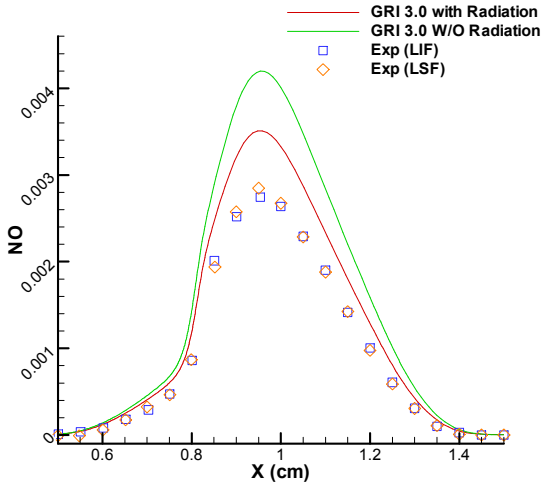

Figure 4. NO mole fraction variation with distance from fuel side for flame C3. Lines represent numerical results of simulation by GRI 3.0 mechanism and symbols represent experimental results of Naik et al. [2002a].

Effect of Chemical Kinetics Model Three mentioned reaction mechanisms have been used to investigate effects of chemical kinetics. In addition, experimental results from Naik et al. [2002a] for flame C4 are plotted for better judgment. Fig 5 shows upper part of temperature profile resulting from mentioned reaction mechanisms. San Diego mechanism predicts the highest value for temperature peak and GRI 2.11 predicted the lowest one. Generally, discrepancy between temperature results is less than 2% and seems acceptable. Fig 6 shows NO variation and again San Diego predicts the highest value for NO. On the other side, surprisingly GRI 3.0 shows the least value. Comparing to experimental results, all reaction mechanisms overstate NO production. Among mechanisms, GRI 3.0 shows better agreement while it still predicts NO about 20% more than experimental results. Consequently, all NO prediction by using these three reaction mechanisms should be taken with some considerations.

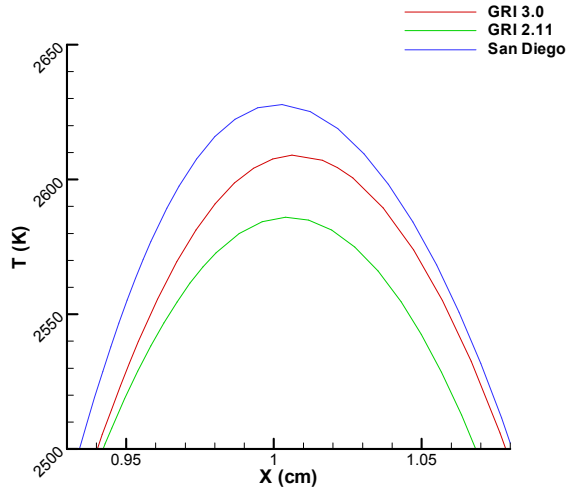

Figure 5. Temperature variation with distance from fuel side for flame C4. Lines represent numerical results of simulation by GRI 3.0, GRI 2.11, and San Diego mechanisms.

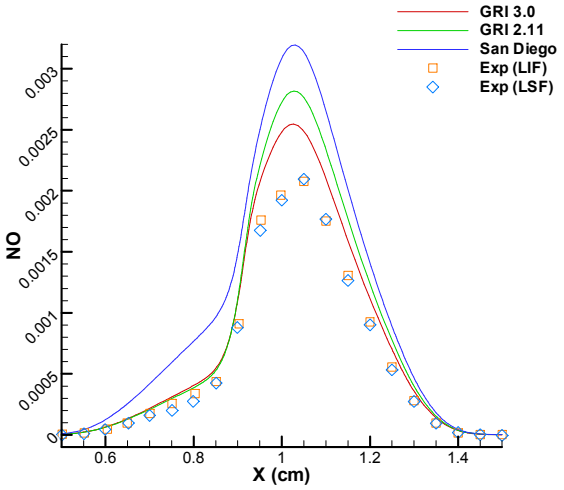

Figure 6. NO mole fraction vs. distance from fuel side for flame C4. Lines show numerical results of simulation by GRI and San Diego mechanisms and symbols show experimental results of Naik et al. [2002a].

Effect of Diffusion Model OPPDIF program has options to model transport properties of gas mixture by using two different methods; multicomponent and mixture-averaged models (see equations 8 to 10). In addition, it can comprise Soret effect in computations of the molecular transport model. Fig 7 presents temperature profiles for four situations. Among them, mixture averaged model including Soret effect predicts the highest value while multicomponent model shows the least peak value. Generally, mixture averaged model predicts higher values for temperature while including Soret effect results in increase in temperature. These behaviors would become more interesting in NO profile (Fig 8). Again, all numerical simulations overestimate peak value of NO. Mixture averaged model shows the worst results and multicomponent model prepares results that are more accurate. Consequently, it could be suggested to use multicomponent model in NO computations in discussed flames.

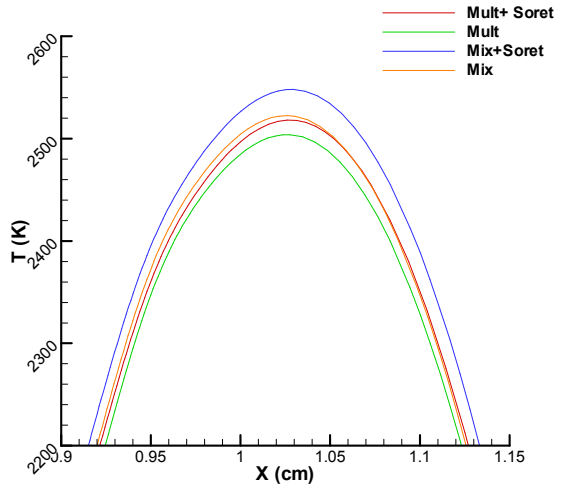

Figure 7. Temperature variation with distance from fuel side for flame C5. Lines represent numerical results of simulation by GRI 3.0 with different diffusion models.

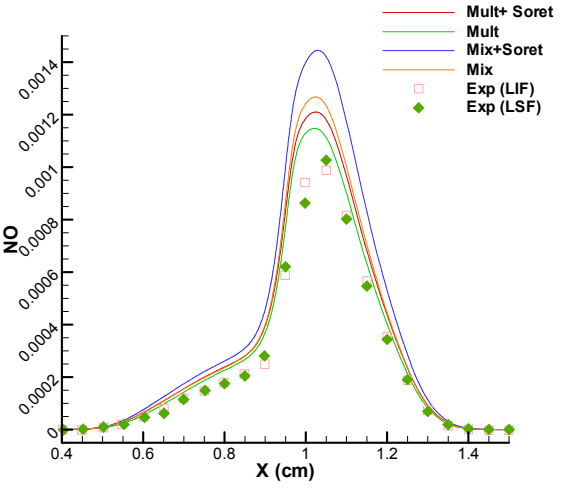

Figure 8. NO mole fraction vs. distance from fuel side for flame C5. Lines show numerical results of simulation by GRI 3.0 with different diffusion models and symbols

show experimental results of Naik et al. [2002a].

CONCLUSION

We performed a parametric study on counterflow flamelet properties in oxygen-enhanced conditions with using OPPDIF program from Chemkin-III collection. Effects of radiation have been investigated by way of enabling appropriate options in OPPDIFF. Results indicate that radiation plays an important role in formation of NO in mentioned flames. Therefore, in relevant simulations this effect should be considered for more realistic results. Additionally, effect of two major molecular diffusion models on NO production has been studied. Multicomponent model showed better agreement to experimental results. Although this model increases time of computation considerably, its effect on NO behavior should be considered and is not negligible. Finally, effect of implementation of different reaction mechanisms has been investigated. Among GRI2.11, GRI3.0, and San Diego mechanisms, GRI3.0 predicted amount of NO more accurately. In general, all performed numerical modeling overstated NO value. Due to strong validation of OPPDIFF program, it seems that more studies on chemical kinetics mechanisms is required to obtain more realistic results.

NOMENCLATURE

a_S	Global strain rate	V_k	Diffusion velocity of the k'th species
C_P	Constant-pressure specific heat	W_k	Molecular weight of the k'th species
$C_{P,k}$	Constant-pressure specific heat of the k'th species	x	Axial location
$D_{k,j}$	Ordinary multicomponent diffusion coefficient of the k'th species in the j'th species	X_k	Mole fraction of the k'th species
D_{km}	Mixture-averaged diffusion coefficients	Y_k	Mole fraction of k'th species
D_k^T	Thermal diffusion coefficient of the k'th species		***Greek symbols***
h_k	Specific enthalpy of the k'th species	$\Delta_{j,k}$	Binary diffusion coefficient of the k'th species in the j'th species
k_P	Plank mean absorption coefficient	σ	Boltzmann constant
L	Distance between two nozzles	μ	Mixture viscosity
P	Pressure	ρ	Mass density
R	Universal gas constant	$\dot{\omega}_k$	Chemical production rate of the k'th species
r	Radial location	ϕ	Equivalence ratio
T	Temperature	λ	Thermal conductivity
T_∞	Environment temperature		***Subscripts***:
u	Axial velocity	O	Oxidant side
v	Radial velocity	F	Fuel side

REFERENCES

Barlow, R.S., Karpetis, A.N., Frank, J.H. [2001], Scalar Profiles and NO Formation in Laminar Opposed-Flow Partially Premixed Methane/Air Flames, *Combustion and Flame*, Vol. 127, pp. 2102-2118.

Baukal, C.E. [1999], *Oxygen Enhanced Combustion,* CRC Press.

Beltrame, A., Porshnev, P., Merchan-Merchan, W., Saveliev, A., Fridman, A., Kennedy, L.A., Petrova, O., Zhdanok, S., Ammouri, F., and Charon, O. [2001], Soot and NO Formation in Methane-Oxygen Enriched Diffusion Flames, *Combustion and Flame*, Vol. 124, pp. 295-310.

Bowman, C. T., Hanson, R. K., Davidson, D. F., Gardiner, W. C. Jr., Lissinsky, V., Smith, G. P., Golden, D. M., Frenklach, M., and Goldenberg, M. [1999], GRI-Mech Homepage, http://www.me.berkeley.edu/gri_mech/

Cheng, Z., Wehrmeyer J.A. and Pitz R.W. [2006], Experimental and Numerical Studies of Opposed Jet Oxygen-Enhanced Methane Diffusion Flames, *Combustion Science and Technology*, Vol. 178, pp. 2145-2163.

Hashemi, H., Soroudi, M.A.and Mazaheri K . [2009],A Numerical Study of Pressure Effects on Methane-Air Partially Premixed Flames, 17th Annual (International) Conference on Mechanical Engineering- ISME2009, University of Tehran, Tehran, Iran

Kee, R. J., Rupley, F. M., Miller, J. A., Coltrin, M. E., Grcar, J. F., Meeks, E., Moffat, H. K., Lutz, A. E., Dixon-Lewis, G, Smooke, M. D., Warnatz, J., Evans, G. H., Larson, R. S., Mitchell, R. E., Petzold, L. R., Reynolds, W. C., Caracotsios, M., Stewart, W. E., Glarborg, P., Wang, C., Adigun, O., Houf, W. G., Chou, C. P., Miller, S. F. [2003], Chemkin Collection, Release 3.7.1, Reaction Design, Inc., San Diego, CA.

Kuligowski, F.F., and Laurendeau, N.M. [1997], Effect of Oxygen Content on NO_X Emission Index for Nonpremixed CH_4-O_2/N_2 Flames, *Combustion Science and Technology*, Vol. 130, pp. 423.

Naik, S.V. and Laurendeau, N.M. [2002a], Laser-Saturated and Linear Laser-Induced Fluorescence Measurements of Nitric Oxide in Counterflow Diffusion Flames under Non-Sooting Oxygen-Enriched Conditions, *Combustion Science and Technology*, Vol. 174, pp. 1-21.

Naik, S.V. and Laurendeau, N.M. [2002b], Quantitative Laser-Saturated Fluorescence Measurements of Nitric Oxide in Counter-Flow Diffusion Flames under Sooting Oxy-Fuel Conditions, *Combustion and Flame*, Vol. 129, pp. 112-119.

Naik, S.V., Laurendeau, N.M., Cooke, J.A., and Smooke, M.D. [2003], Effect of Radiation on Nitric Oxide Concentration under Sooting Oxy-Fuel Conditions, *Combustion and Flame*, Vol. 134, pp. 425-431.

NETL Report [2004], Carbon Sequestration: Technology Roadmap and Program Plan - 2004.

Soroudi, M.A. and Fakhr-Tabatabaei, A. [2006], Numerical Investigation of Partial Premixing and Hydrogen Addition Effects on Natural Gas Combustion Pollutants Reduction, 10th Fluid Dynamics Conference, Yazd University, Yazd, Iran (in Persian).

Sung, C.J. and Law, C.K. [1998], Dominant Chemistry and Physical Factors Affecting NO Formation and Control in Oxy-Fuel Burning, *Proceedings of the Combustion Institute*, Vol. 27, pp. 1411-1418.

Wang, L., Haworth, D.C., Turns, S.R., Modest, M.F. [2005], Interactions among Soot, Thermal Radiation, and NO_X Emissions in Oxygen-Enriched Turbulent Nonpremixed Flames: A Computational Fluid Dynamics Modeling Study, *Combustion and Flame*, Vol. 141, pp. 170-179.

Williams, F.A. [2000], Progress in Knowledge of Flamelet Structure and Extinction, *Progress in Energy and Combustion Science*, Vol. 26, pp. 657-682.

Williams, F. A. [2005], Chemical-Kinetic Mechanisms for Combustion Applications [online], University of California, San Diego, Available from: http://maeweb.uscd.edu/~combustion/cermech [Accessed August 2009].